IOP Conf. Series: Materials Science and Engineering **678** (2019) 012025 doi:10.1088/1757-899X/678/1/012025

A Novel Technique for the Measurement of the Effective Thermal Conductivity of Thermal Insulating Materials up to 1000°C

Zenghua Gao*, Yang Wang, Jinshuai Zhou, Tao Yuan, Xian Wu

Aerospace Advanced Materials and Processing Technology Institute, Beijing, China

* zhgao@alum.imr.ac.cn

Abstract. A novel large temperature gradient steady-state technique for the measurement of the effective thermal conductivity of thermal insulating materials up to 1000°C has been developed. With the incorporation of a vacuum system, the mean effective thermal conductivity of thermal insulating materials under certain temperature gradient in air and/or inert atmospheres with the gas pressure range of 10^{-2} Pa to 10^{5} Pa can be measured. A transforming method was proposed to derive the true effective thermal conductivity from the as-measured mean effective thermal conductivity. By evaluating the measurement uncertainty of the constructed testing apparatus as well as comparing experimentally with the guarded hot plate test results, the measurement accuracy of this technique was determined to have an accuracy of less than 8.5%.

1. Introduction

Thermal insulating materials have been widely used in many industries related to high temperature applications, such as aerospace thermal protection systems (TPS)[1-4], refractories for industrial furnaces and metallurgical engineering[5,6], etc. Since heat conducting ability is one of the most concerned properties for the design and selection of thermal insulating materials, the accurate evaluation of their effective thermal conductivity under certain thermal environments is of great importance.

A plenty of methods and techniques for the measurement of thermal conductivity of materials have been developed. Generally, it can be divided into two different categories[7], steady-state methods and transient methods, according to the time-independence/-dependence of the temperature field in the material. For thermal insulating materials, the transient methods are normally not preferred, in that the theoretical boundary conditions are difficult to be fully satisfied and the as-resulted errors are difficult to evaluate. In comparison, the steady-state methods, based on Fourier’s law of heat conduction, can be simply described and applied with superior reliability and accuracy. However, for the accurate evaluation of advanced insulation materials applied in high temperature environments, especially with large temperature gradient and/or certain gas pressures, the current steady-state methods have their limits. Table 1 lists the application scopes and limits of typical steady-state methods for thermal insulating materials [8-11]. As an absolute steady-state method for arbitration, the guarded hot plate (GHP) method has rigorous requirements in the design and construction of the test system to maintain its accuracy. Until now, the highest reported practical application temperature using this method is 800°C, realized by the high temperature GHP apparatus developed in National Physical Laboratory (NPL) in UK[12,13]. Heat flow meter (HFM) method is a comparative steady-state one and needs to be calibrated using standard reference specimens with known thermal transmission properties. The lack of high temperature standard reference insulation materials restricts its application at high temperatures[12]. Water-flow calorimeter (WFC) method is similar with HFM but measures the heat flow under large temperature gradient directly with a water-flow calorimeter, hence possesses the advantage of high service temperatures for the measurement of refractory bricks. Following this method, ATLIRR[10] (Sinosteel Luoyang Institute of Refractories Research) has developed its PBD-series thermal conductivity testers, with the highest hot side temperature being 1600°C. Gerald Bath *et al*.[11] have also constructed a test facility for effective thermal conductivity measurement up to a hot side temperature of 1650°C. Although it can be applied to high temperatures, however, the coarse design in the heating unit and the susceptible water-flow calorimeter can easily cause large errors, which makes it only suitable for quality control in refractory bricks production.

Table 1. Typical steady-state methods for thermal conductivity measurement of thermal insulating materials

Method	Practical service temperature	Relevant standard*	Main advantage	Main limit
Guarded Hot Plate	-170°C ~ 800°C [8]	ASTM C177 ISO 8302	High accuracy	Low service temperature
Heat Flow Meter	-195°C ~ 540°C [9]	ASTM E1530 ASTM C518 ISO 8301	Easiness in practice	Low service temperature
Water-flow Calorimeter	100°C ~ 1650°C [10,11]	ASTM C201/202/182	High service temperature	Low accuracy

*ASTM: American Society for Testing Materials; ISO: International Organization for Standardization.

To evaluate the effective thermal conductivity of high temperature insulations used for re-entry TPS, NASA Langley Research Center (LaRC) designed a thermal-vacuum testing apparatus with a hot side temperature of 1000°C[14]. Compared to the WFC technique, it optimized the heat flow measurement by using thin film heat flow gauges and added the function for measurement under different gas pressures. Referring to that apparatus in LaRC, He *et al*.[15] constructed a graphite plate heater-based testing facility and declared a highest hot side temperature of 1600 °C in N_2. Unlike the GHP and HFM methods, however, the as-measured results by the above techniques were the mean effective thermal conductivity under various large temperature gradients[11]. Since the thermal conductivity of most insulation materials exhibit non-linear temperature dependence[12], the test results of mean effective thermal conductivity were neither intra-comparable nor inter-comparable.

In this work, a novel large temperature gradient steady-state technique for the measurement of the effective thermal conductivity of thermal insulating materials up to 1000°C in air and/or inert atmospheres with the gas pressure range of 10^{-2} Pa to 10^5 Pa was designed and constructed. And a transforming method was proposed to calculate the true effective thermal conductivity from the as-measured mean effective thermal conductivity. Finally, the measurement accuracy of this technique were analyzed theoretically and experimentally.

2. Design and Construction of the Novel Technique

2.1. Design Principle

The novel large temperature gradient steady-state technique introduced here is also based on the Fourier's law on the unidirectional steady-state heat conduction, as expressed by Eq. 1. When the upper and lower surfaces of a plate specimen, having the surface area, are uniformly maintained at temperatures of T_h and T_c, respectively, there will be a constant heat flux q existing only in the direction of specimen thickness l. At this steady state, by measuring q, the mean effective thermal conductivity of the specimen $\lambda_{e,m}$ under the temperature gradient of (T_h-T_c) can be determined by Eq. 1. Be aware that, the so-obtained $\lambda_{e,m}$ under large temperature gradient represents not the true effective thermal conductivity ($\lambda_{e,t}$) at the average temperature of T_h and T_c.

$$\lambda_{\mathrm{e,m}} = \frac{ql}{T_{\mathrm{h}} - T_{\mathrm{c}}} \tag{1}$$

2.2. Apparatus Construction

Based on the above principle, a testing apparatus LTG-1000 with the ability to conduct the effective thermal conductivity measurements of thermal insulating materials in air and/or inert atmospheres with the gas pressure range of 10^{-2} Pa to 10^5 Pa was constructed. With the large temperature gradient steady-state technique, it enables to reach a highest hot surface temperature no less than 1000°C, while maintaining the cold surface of the specimen at below 50°C. The main structure of the LTG-1000 is schematically illustrated in Figure 1. It generally consists of six units: specimen, the heating unit, the cooling unit, the thermal insulation unit, the laser displacement sensor unit and the vacuum unit.

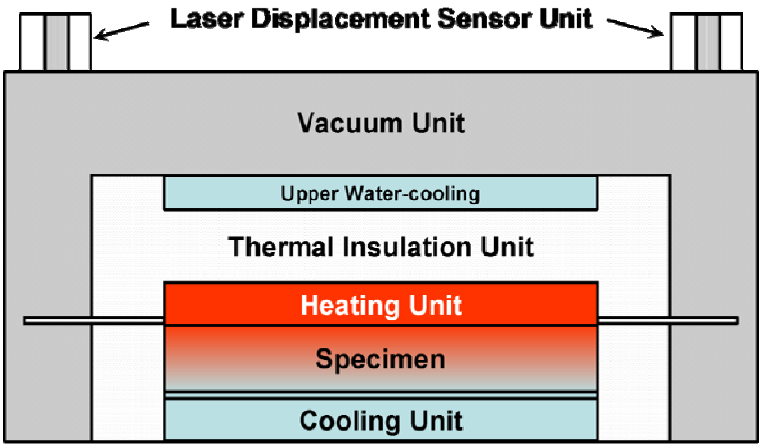

Figure 1. Schematic drawing of the main structure of the testing apparatus LTG-1000 developed in this work.

2.2.1 Specimen. For this technique, single 300 mm×300 mm square-shaped plate specimen is needed. And the preferred thickness of the specimen is 10 mm to 30 mm, mainly considering together the minimization of the lateral heat dissipation of the specimen and the weakening of the influence of the contact thermal resistance.

2.2.2 Heating unit. Figure 2 shows in detail the structure of the designed heating unit. Its main functions are: provide constantly a uniform thermal distribution no less than 1000°C on and across the metered region of the specimen, meanwhile, directly and accurately measure that temperature distribution. To fulfill these aims, several parts of this unit were carefully designed. First and foremost, a plate radiation heater, made of FeCrAl alloy, was designed with an overall size of 300 mm × 300 mm × 2.5 mm and mounted above the heat uniformizer by several ceramic supports. The heater consists of a single circuit and has a special homocentric square frame configuration, in which the spacing between each square frame is descending from inside to outside. This configuration ensures, from the first step, a well uniformity of heat radiation onto the 100 mm × 100 mm metered region of the heat uniformizer. Secondly, a 300 mm × 300 mm × 10 mm plate heat uniformizer, made of 310S stainless steel, was used to further reduce the heat nonuniformity. To release the thermal stress and to alleviate the bowing due to the residual temperature nonuniformity on this plate, four slots were machined, as is shown in Figure 2(b). The heat uniformizer also bears the entire weight of the heating unit through four ceramic pullrods. Last but not the least, to directly monitor the temperature distribution on the top surface of the specimen and to minimize the influence of the thermocouple wiring at the same time, 12 type-K thermocouples were needled through the upper thermal insulation unit, the heater and the heat uniformizer, to contact directly with the top surface of the specimen. Figure 2(b) shows the location array of the 12 thermocouples, including 8 in the central metered region.

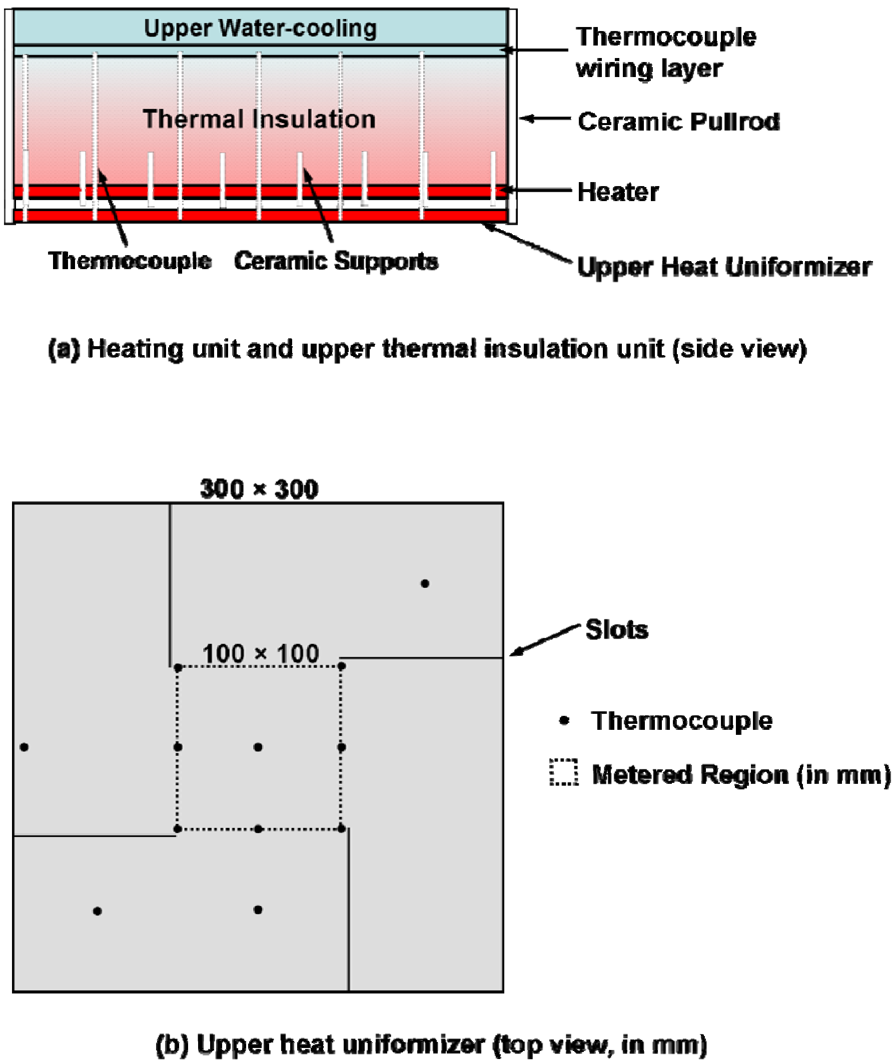

Figure 2. Detailed schematic drawing of the heating unit of LTG-1000.

2.2.3 Cooling unit. Figure 3 shows in detail the structure of the designed cooling unit. Having the symmetrical structure with the heating unit, the main functions of the cooling unit are: keep the bottom surface of specimen at a uniform temperature of no more than 50°C, in the meantime, monitor the temperature distribution and the heat flow conducted downward. To achieve that, firstly, an Al-alloy plate cyclically cooled by silicon oil was used as the cooler, and a copper alloy heat uniformizer (with a thermal conductivity of ~120 W/m·K at room temperature) was put onto the cooler plate to further facilitate the temperature distribution. In between those two plates locates a total of 7 thin film heat flux sensors (HFS-4, OMEGA, USA), 5 in the metered region, whose locations are schematically shown in Figure 3(b). With the thickness of less than 0.3 mm, these sensors were mounted into a thin layer of thermal conductive silicon grease and could measure the heat flow and temperature simultaneously.

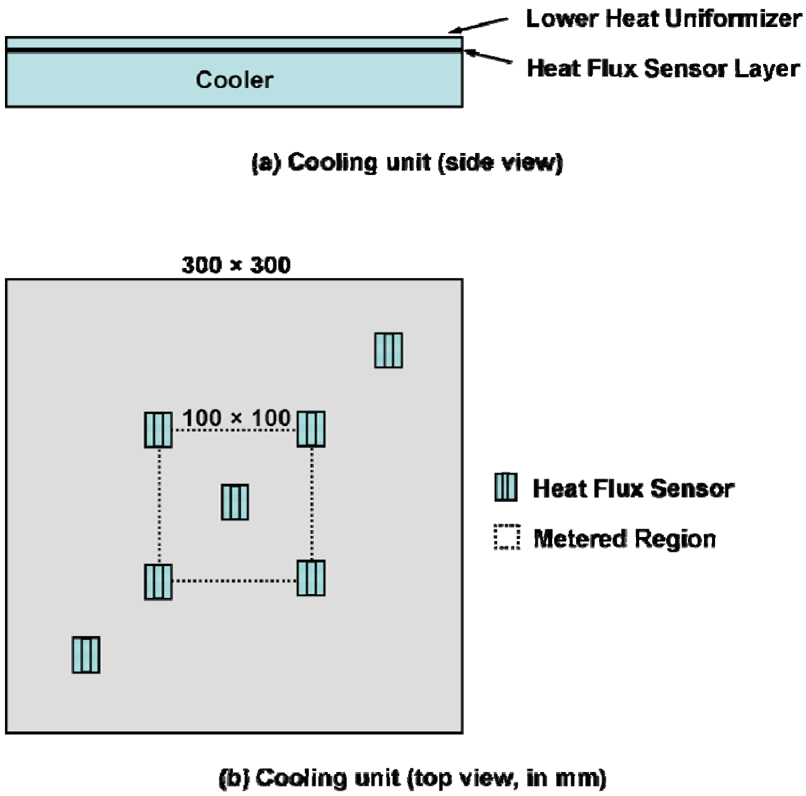

Figure 3. Detailed schematic drawing of the cooling unit of LTG-1000.

2.2.4 Thermal insulation unit. The four lateral sides of the heating unit, specimen and the cooling unit are all covered by high temperature insulation. In combination with the design of the heating and cooling units, it is indispensable to help in producing a steady unidirectional heat flow through the specimen. The upper side of the heater is also covered by high temperature insulation, which not only takes effect in ensuring heating efficiency but also provides needling tunnels for thermocouples.

2.2.5 Vacuum unit. To evaluate the effective thermal conductivity of thermal insulation materials in low gas pressure environments, a vacuum unit was designed and incorporated into the testing apparatus. It is mainly composed of vacuum chamber, vacuum pump, gas supplier and gas pressure regulator. With that, testing environments of 10^{-2} Pa to 10^{5} Pa in air and/or inert atmosphere can be realized.

2.2.6 Laser displacement sensor unit. For the test at gas pressures below 1 atm, the thickness of the specimen might be different from that at ambient pressure, especially for non-rigid materials, such as insulating fabrics. Therefore, two laser displacement sensors are mounted at two countering sides of the vacuum chamber to measure the thickness change of the specimen by monitoring the distance change between the upper and lower heat uniformzier *in situ*.

3. Transforming $\lambda_{e,m}$ To $\lambda_{e,t}$

As mentioned above, the as-measured results by large temperature gradient steady-state technique are actually the mean effective thermal conductivity, $\lambda_{e,m}$, in the temperature range of T_c~T_h, but not the true effective thermal conductivity, $\lambda_{e,t}$, at a set temperature. For most materials with non-linear thermal conductivity *vs.* temperature relationship, different temperature gradients applied on specimen during testing might produce the same mean temperature but different measurement results, meaning that the test results were neither intra-comparable nor inter-comparable. Therefore, a transformation of $\lambda_{e,m}$ to $\lambda_{e,t}$ is of great necessity.

According to Eq. 1 and its partial differential form for unidirectional steady-state heat conduction, as described by Eq. 2, the relationship between $\lambda_{e,m}$ and $\lambda_{e,t}$ can be derived as Eq. 3.

$$\lambda_{e,t} = -q\frac{dl}{dT} \tag{2}$$

$$\lambda_{e,m} = \frac{\int_{T_c}^{T_h} \lambda_{e,t}\, dT}{T_h - T_c} \tag{3}$$

Since the thermal conductivity of most materials have n-order (n=0, 1, 2, ..., N) polynomial relationship with temperature[12], $\lambda_{e,t}$ can be presented by Eq. 4, where a_n is the coefficient of each term. Substituting Eq. 4 into Eq. 3 and conducting integration, the relationship between $\lambda_{e,m}$ and $\lambda_{e,t}$ can be rewritten as Eq. 5. In this equation, only a_n is the unknown, which can be solved mathematically by iterating n groups of different $\lambda_{e,m}$, T_h and T_c values. With a_n being solved, the polynomial relationship of $\lambda_{e,t}$ with temperature is determined.

$$\lambda_{e,t} = \sum_{n=0}^{N} a_n T^n \tag{4}$$

$$\lambda_{e,m}(T_h - T_c) = \sum_{n=0}^{N} \frac{T_h^{n+1} - T_c^{n+1}}{n+1} a_n \tag{5}$$

4. Evaluation of Measurement Accuracy

Though the theoretical basis of this technique is very simple, to transfer it into testing apparatus with high measurement accuracy is somehow technically uneasy. All the factors relevant to the measurement of each parameter appeared in the right side of Eq. 1 result in the measurement errors of the mean effective thermal conductivity. In this regard, the measurement accuracy of this technique were determined both forwardly using measurement uncertainty evaluation and reversely by experimental comparison.

4.1. *Measurement uncertainty evaluation*

According to ISO/IEC GUIDE 98-3:2008(E)[16], the expanded combined relative standard measurement uncertainty of $\lambda_{e,m}$, $\frac{U_C(\lambda_{e,m})}{\lambda_{e,m}}$, can be expressed by the following Eq. 6.

$$\frac{U_C(\lambda_{e,m})}{\lambda_{e,m}} = k\frac{u_C(\lambda_{e,m})}{\lambda_{e,m}} = k\sqrt{\frac{u_A^2(\bar{\lambda}_{e,m})}{\bar{\lambda}_{e,m}^2} + \frac{u_B^2(\lambda_{e,m})}{\lambda_{e,m}^2}} \tag{6}$$

In which, $\bar{\lambda}_{e,m}$ represents the average $\lambda_{e,m}$ from repeated tests, k is coverage factor, $u_A(\bar{\lambda}_{e,m})$ and $\frac{u_A(\bar{\lambda}_{e,m})}{\bar{\lambda}_{e,m}}$ are the type A standard uncertainty and type A relative standard uncertainty of $\bar{\lambda}_{e,m}$, $u_B(\lambda_{e,m})$ and $\frac{u_B(\lambda_{e,m})}{\lambda_{e,m}}$ are the type B standard uncertainty and type B relative standard uncertainty of $\lambda_{e,m}$, respectively.

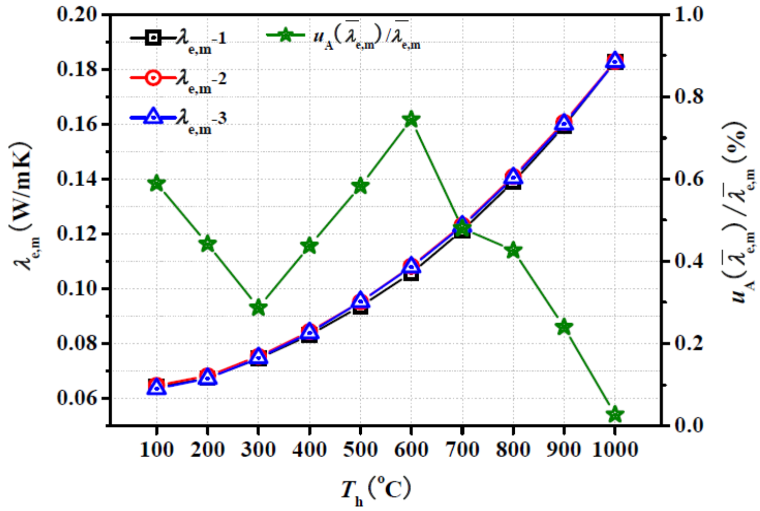

Figure 4. Experimental results of a high temperature insulation material in ambient air at hot surface temperatures of 100°C ~ 1000°C using LTG-1000.

Table 2. Experimental results of a high temperature insulation material in ambient air at hot surface temperatures of 100°C ~ 1000°C using LTG-1000

Hot surface temperature, T_h (°C)	Mean effective thermal conductivity (W/m·K)				Standard deviation, $s(\lambda_{e,m})$ (W/m·K)	Type A relative standard uncertainty (%)
	$\lambda_{e,m}$-1	$\lambda_{e,m}$-2	$\lambda_{e,m}$-3	$\bar{\lambda}_{e,m}$		
100	0.06419	0.06485	0.06354	0.06419	0.00066	0.59
200	0.06744	0.06824	0.06727	0.06765	0.00052	0.45
300	0.07457	0.07531	0.07486	0.07491	0.00037	0.29
400	0.08315	0.08441	0.08393	0.08383	0.00064	0.44
500	0.09358	0.09520	0.09527	0.09468	0.00096	0.59
600	0.10572	0.10828	0.10791	0.10730	0.00138	0.75
700	0.12129	0.12322	0.12282	0.12244	0.00102	0.48
800	0.13894	0.14094	0.14040	0.14009	0.00103	0.43
900	0.15937	0.16070	0.16000	0.16002	0.00067	0.24
1000	0.18287	0.18293	0.18276	0.18285	0.00009	0.03

4.1.1 $\dfrac{u_A(\bar{\lambda}_{e,m})}{\bar{\lambda}_{e,m}}$**.** To estimate $\dfrac{u_A(\bar{\lambda}_{e,m})}{\bar{\lambda}_{e,m}}$, the mean effective thermal conductivity of a high temperature insulation material was taken as an example and measured repeatedly on LTG-1000 in ambient air at T_h of 100 °C~1000 °C with the interval of 100°C for 3 times. The results are summarized in Figure 4 and Table 2, in which $s(\lambda_{e,m})$ represents the experimental standard deviation of $\lambda_{e,m}$. According to $u_A(\bar{\lambda}_{e,m}) = s(\lambda_{e,m})/\sqrt{3}$, the $\dfrac{u_A(\bar{\lambda}_{e,m})}{\bar{\lambda}_{e,m}}$ of the experimental result at each hot surface temperature was obtained. It can be seen that, the $\dfrac{u_A(\bar{\lambda}_{e,m})}{\bar{\lambda}_{e,m}}$ in the whole hot surface temperature range has the maximum value of 0.75% .

4.1.2 [$u_B(\lambda_{e,m})/\lambda_{e,m}$]. According to Eq. 1, $u_B(\lambda_{e,m})$ has several uncorrelated components, which can be expressed as Eq. 7.

$$\frac{u_B(\lambda_{e,m})}{\lambda_{e,m}} = \sqrt{\frac{u^2(q)}{q^2} + \frac{u^2(d)}{d^2} + \frac{u^2(T_h)}{(T_h - T_c)^2} + \frac{u^2(T_c)}{(T_h - T_c)^2}} \tag{7}$$

Where, $u(q)$, $u(T_h)$, $u(T_c)$ and $u(d)$ are the standard measurement uncertainties of Q, T_h, T_c, and d, respectively.

Table 3. Evaluation of type B relative standard measurement uncertainty in LTG-1000

Measured	Sensor accuracy (%)	Maximum measurand distribution error in the metered region (%)	Combined relative standard uncertainty (%)
Heat flux, q	1.62	5.45	3.15
Hot surface temperature, T_h	0.50	3.91	2.26
Cold surface temperature, T_c	0.50	1.30	0.81
Thickness, d	0.02	0.07	0.05
Type B relative standard measurement uncertainty, $\frac{u_B(\lambda_{e,m})}{\lambda_{e,m}}$ (%)			3.96

The uncertainty of q (the same for T_h, T_c, and d) in LTG-1000 is combined by the accuracy of each heat flux sensor (hot surface thermocouple, cold surface thermocouple and laser displacement sensor) and the heat flux distribution (hot surface temperature distribution, cold surface temperature distribution and thickness distribution) error in the metered region. Besides, the uncertainty of T_c also includes the influence of the copper lower heat uniformizer. The accuracy of various sensors were determined by standard calibrations, while the maximum distribution errors of these measurands were experimentally estimated. Table 3 lists all the estimation results of type B standard measurement uncertainty components in LTG-1000. It should be noted that the sensor accuracy and the measurand distribution error were all considered to obey uniform distribution.

4.1.3 [$u_C(\lambda_{e,m})/\lambda_{e,m}$]. Substituting the estimation results of type A and type B relative standard uncertainties into Eq. 6, the combined relative standard measurement uncertainty of $\lambda_{e,m}$ using LTG-1000, [$u_C(\lambda_{e,m})/\lambda_{e,m}$], was determined to be 4.03%.

4.1.4 [$u_C(\lambda_{e,m})/\lambda_{e,m}$]. According to [$u_C(\lambda_{e,m})/\lambda_{e,m}$], the expanded combined relative standard measurement uncertainty of $\lambda_{e,m}$ was determined to be 8.06% with $k = 2$.

4.2. Experimental comparison

Using a reference calcium silicate insulation material (Density: 0.74 g/cm^3), the measurement accuracy of the LTG-1000 testing apparatus developed in this work was experimentally assessed by comparing to a GHP testing apparatus, NETZSCH 456 Titan®, from 100 ^{o}C up to 600 ^{o}C in ambient air. The results are shown in Figure 5 and Table 4, respectively. It should be noted that the as-measured $\lambda_{e,m}$ results using LTG-1000 were transformed to $\lambda_{t,m}$ before comparison using the proposed transforming method in this work. It can be seen that, compared to the GHP result, the LTG-1000 result exhibits a relative error of 1.16%~8.37%.

It can be acknowledged from the above analysis that, the results of the measurement uncertainty evaluation and the experimental comparison have a well agreement. Since some minor factors, such as the contact quality of various sensors with the specimen surface, which also contribute to the measurement uncertainty, were not analyzed, it is believed that the LTG-1000 developed in this work exhibits an overall measurement accuracy of less than 8.5%.

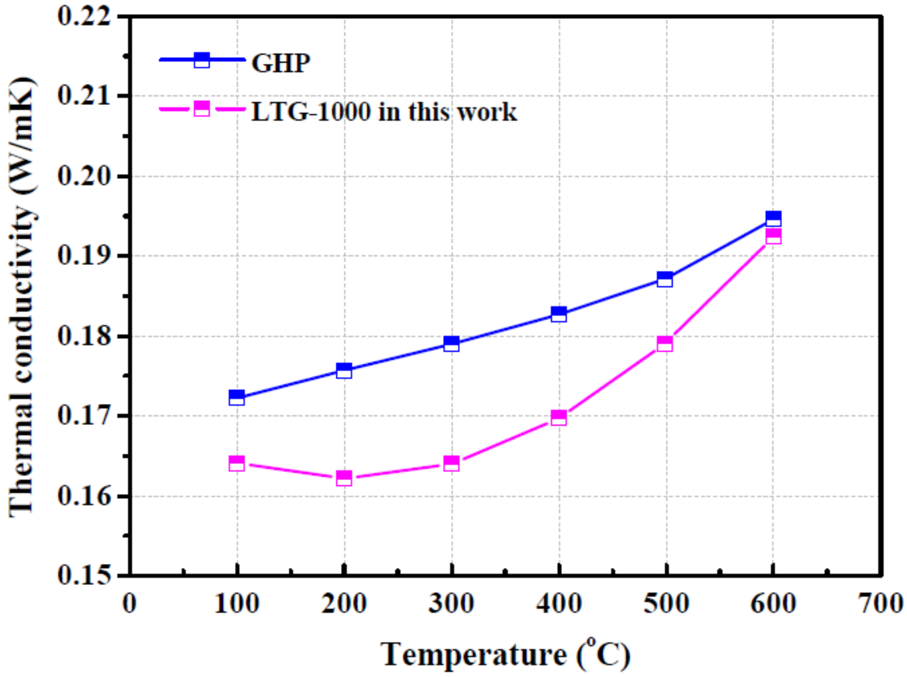

Figure 5. Experimental comparison between the guarded hot plate (GHP) method and the large gradient temperature technique (LTG-1000) developed in this work, using the testing results of a calcium silicate insulation material at 100 °C~600 °C in ambient air.

Table 4. Experimental comparison between the guarded hot plate (GHP) method and the large gradient temperature technique (LTG-1000) developed in this work, using the testing results of a calcium silicate insulation material at 100 °C~600 °C in ambient air

Temperature (°C)	Experimental results of thermal conductivity (W/m·K)		Relative error (%)
	GHP	LTG-1000	
100	0.17224	0.16413	4.71
200	0.17570	0.16219	7.69
300	0.17902	0.16404	8.37
400	0.18269	0.16968	7.13
500	0.18715	0.17912	4.30
600	0.19461	0.19236	1.16

5. Conclusions

Based on the Fourier’s law on the unidirectional steady-state heat conduction, a novel large temperature gradient steady-state testing apparatus for the evaluation of the effective thermal conductivity of thermal insulating materials up to 1000 °C in air and/or inert atmospheres with the gas pressure range of 10^{-2} Pa to 10^{5} Pa was designed and constructed. For better comparability and measurement accuracy evaluation of the as-measure results, a transforming method was proposed to derive the true effective thermal conductivity from the as-measured mean effective thermal conductivity. According to the analysis by the standard measurement uncertainty evaluation and the experimental comparison with the guarded hot plate method, the testing apparatus developed in this work exhibits a measurement accuracy of less than 8.5%.

IOP Conf. Series: Materials Science and Engineering **678** (2019) 012025 doi:10.1088/1757-899X/678/1/012025

References

[1] Daryabeigi K 1999 *Effective Thermal Conductivity of High Temperature Insulations for Reusable Launch Vehicles* NASA/TM-1999-208972
[2] Zhang B, Zhao S, He X and Du S 2007 *J. Mater. Sci. Technol.* **23** 860
[3] Feng J, Gao Q F, Feng J Z and Jiang Y G 2010 *J. National Univ. of Def. Technol.* **32** 40
[4] Sun J, Hu Z, Chen H, Wang Q and Wang X 2012 *Aerospace Mater.Technol.* **42** 93
[5] Kandell B 2009 *Key Engineering Materials* **395** 143
[6] Wang S, Gu N, Miao W, Cheng G, *et al.* 2009 *Rare Metal Mater. Eng.* **38** 1259
[7] Yang SM, Tao WQ 2012 *Heat transfer* 4th ed, Higher Education Press, Beijing
[8] Information on http://www.npl.co.uk
[9] Standard test method for steady-state thermal transmission properties by means of the heat flow meter apparatus, ASTM C201-93 (2013)
[10] Information on http://www.atlirr.com
[11] Barth G, Gross U and Wulf R 2007 *Inter. J. Thermophys.* **28** 1668
[12] Salmon D 2001 *Meas. Sci. Technol.* **12** R89
[13] Wu J, Salmon D, Lockmuller N and Stacey C 2010 *Desigh, construction and performance checks of the NPL upgraded high temperature guarded hot plate* Proceedings of the Thirtieth International Thermal Conductivity Conference, pp. 529
[14] Daryabeigi K 2010 *Heat transfer modeling and validation for optically thick alumina fibrous insulation* Proceedings of the Thirtieth International Thermal Conductivity Conference, pp. 120
[15] He F, He X and Zhao S 2007 *Aerospace Mater. Technol.* **37** 67
[16] Uncertainty of measurement Part 3: Guide to the expression of uncertainty in measurement (GUM:1995), ISO/IEC GUIDE 98-3 (2008).